Analysis of the Reaction Force for a Gas Phase S_N2 Process: $CH_3Cl + H_2O \rightarrow CH_3OH + HCl$†

Peter Politzer,*,‡ Jaroslav V. Burda,§ Monica C. Concha,‡ Pat Lane,‡ and Jane S. Murray‡

Department of Chemistry, University of New Orleans, New Orleans, Louisiana 70148, and Department of Chemical Physics and Optics, Faculty of Mathematics and Physics, Charles University, Ke Karlovu 3, 121 16 Prague, Czech Republic

Received: July 14, 2005

The "reaction force" $\mathbf{F}(\mathbf{R}_c)$ is the negative derivative of a system's potential energy $V(\mathbf{R}_c)$ along the intrinsic reaction coordinate of a process. If $V(\mathbf{R}_c)$ goes through a maximum, as is commonly the case, then $\mathbf{F}(\mathbf{R}_c)$ has a characteristic profile: a negative minimum followed by zero at the transition state and then a positive maximum. These features reflect four phases of the reaction: an initial one of reactant preparation, followed by two of transition to products, and then relaxation of the latter. In this study, we have analyzed, in these terms, a gas-phase S_N2 substitution, selected to be $CH_3Cl + H_2O \rightarrow CH_3OH + HCl$. We examine, at the B3LYP/6−31G* level, the geometries, energetics, and molecular surface electrostatic potentials, local ionization energies, and internal charge separation.

Introduction

For any chemical process, the potential energy $V(\mathbf{R}_c)$ of the system along the intrinsic reaction coordinate $\mathbf{R}_c$[1,2] has an associated "reaction force" $\mathbf{F}(\mathbf{R}_c)$, defined by

$$\mathbf{F}(\mathbf{R}_c) = -\frac{\partial V(\mathbf{R}_c)}{\partial \mathbf{R}_c} \tag{1}$$

In the commonly observed case in which $V(\mathbf{R}_c)$ passes through a maximum, as in Figure 1a, $\mathbf{F}(\mathbf{R}_c)$ has the general features shown in Figure 1b. It is zero for the reactants and products, has a negative minimum at the first inflection point of $V(\mathbf{R}_c)$, has a positive maximum at the second, and is zero for the transition state. These characteristics of $\mathbf{F}(\mathbf{R}_c)$ are universal, independent of the specific process and whether it is exo- or endoenergetic, as long as $V(\mathbf{R}_c)$ has a maximum. In the reverse reaction, $\mathbf{R}_c$ increases in the opposite direction and $\mathbf{F}(\mathbf{R}_c)$ is the negative of that in Figure 1b.

The significance and interpretation of the reaction force has been investigated in a series of recent studies.[3−9] The minimum, zero, and maximum of $\mathbf{F}(\mathbf{R}_c)$ identify three key points along the intrinsic reaction coordinate, labeled α, β, and γ in Figure 1b. These establish four zones along $\mathbf{R}_c$: reactants (R) $\rightarrow \alpha$, $\alpha \rightarrow \beta$ (transition state), $\beta \rightarrow \gamma$, and $\gamma \rightarrow$ products (P). In the first of these, R $\rightarrow \alpha$, $\mathbf{F}(\mathbf{R}_c)$ is a retarding force, which increases until $\mathbf{R}_c = \alpha$. At this point it begins to diminish, presumably because a driving force has begun to be felt. The two exactly balance at the transition state, $R_c = \beta$, after which the driving force dominates and continues to become stronger until $R_c = \gamma$, whereupon it begins to weaken, and is zero at the products.

We have suggested[4−9] that the R $\rightarrow \alpha$ portion of a process is one of preparation, involving mainly structural changes (such as rotations) that will facilitate the subsequent transition to products, which occurs primarily in the zones $\alpha \rightarrow \beta$ and $\beta \rightarrow \gamma$. The last phase, $\gamma \rightarrow$ P, is then a relaxation to the equilibrium states of the products.

This interpretation, and indeed the profile of $\mathbf{F}(\mathbf{R}_c)$, reflects the variation of structural and electronic properties along the intrinsic reaction coordinate. For a series of hydrogen and fluorine transfer processes, we have found that the participating atoms' electrostatic potentials, local ionization energies, atomic charges, Fukui functions and bond orders show a characteristic pattern:[4−9] a slow and gradual increase or decrease in the preparation zone between R and α, a very rapid change in the transition regions $\alpha \rightarrow \beta$ and $\beta \rightarrow \gamma$, and then again slow and gradual as the system relaxes to the products, $\gamma \rightarrow$ P. The rapid change in the property between $R_c = \alpha$ and $R_c = \gamma$ may be monotonic, or it may go through a maximum or minimum at the transition state, $R_c = \beta$. It is important to keep in mind that it is the electronic and structural changes occurring along the intrinsic reaction coordinate that determine the features of $V(\mathbf{R}_c)$ and hence $\mathbf{F}(\mathbf{R}_c)$, not the reverse.

In this work, our objective has been to extend the analysis to a different type of chemical reaction. As an example, we chose the gas-phase S_N2 substitution of Cl by OH:

$$CH_3Cl + H_2O \rightarrow CH_3OH + HCl \tag{2}$$

While H_2O is a less effective nucleophile than, e.g., OH^-,[10] we prefer to use neutral reactants in the present context, since the charge on an ion could distort or mask some of the property variations of interest.

Procedure

All of the computations in this work have been at the density functional B3LYP/6-31G* level. Apart from the energy and the reaction force, the two properties upon which we shall focus are the electrostatic potential $V(\mathbf{r})$ and the average local ionization energy $\bar{I}(\mathbf{r})$; these shall be defined and discussed later in this section. For analyzing chemical reactivity, we have found it useful to calculate $V(\mathbf{r})$ and $\bar{I}(\mathbf{r})$ on the respective molecular

* To whom correspondence should be addressed. E-mail: ppolitze@uno.edu.

† Part of the special issue "Donald G. Truhlar Festschrift".

‡ University of New Orleans.

§ Charles University.

10.1021/jp0582080 CCC: $33.50
Published on Web 10/13/2005

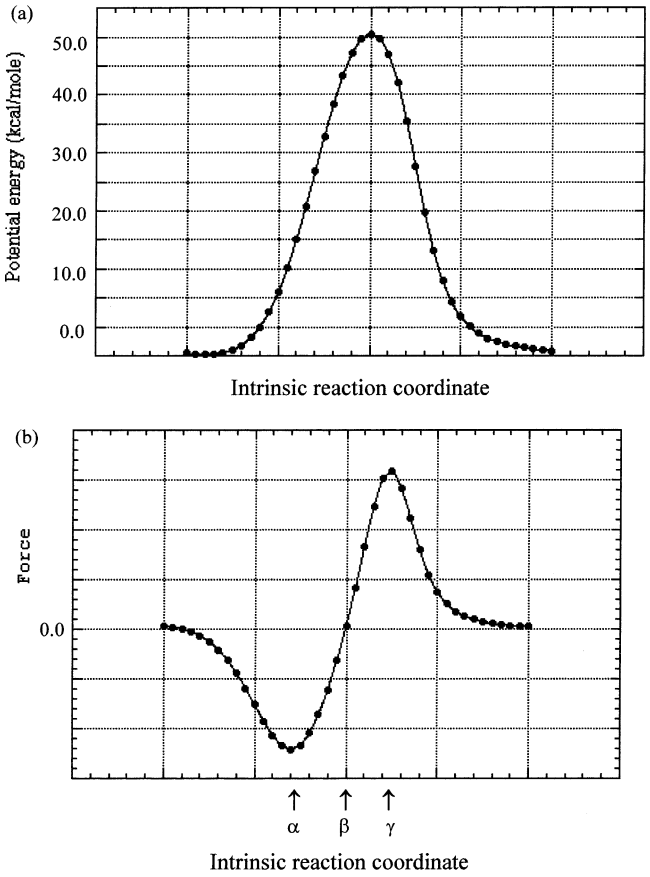

Figure 1. Potential energy $V(\mathbf{R}_c)$ (a) and reaction force $\mathbf{F}(\mathbf{R}_c)$ (b) along the intrinsic reaction coordinate of process in eq 2. The positions of the reaction force minimum and maximum, α and γ, and the transition state, β, are indicated. For practical reasons, these profiles were not extended to the relatively large reactant and product separations at which there would be no CH_3Cl- - - -H_2O and CH_3OH- - - -HCl interactions whatsoever, and $V(\mathbf{R}_c)$ would equal zero. Thus, the $V(\mathbf{R}_c)$ and $\mathbf{F}(\mathbf{R}_c)$ profiles begin at a point where there is already some hydrogen bonding between the reactants, with H_3CCl- - - -HOH and H_2O- - - -HCH_2Cl distances of 2.693 and 2.385 Å, respectively; at their termination, there is still some interaction between the products, the O- - - -H separation being 1.748 Å.

surfaces. These are defined, following Bader et al.,[11] as the 0.001 electrons/bohr^3 contours of the electronic densities.

The electrostatic potential that the electrons and nuclei of a system create at any point in the surrounding space is given by

$$V(\mathbf{r}) = \sum_A \frac{Z_A}{|\mathbf{R}_A - \mathbf{r}|} - \int \frac{\rho(\mathbf{r}')\, d\mathbf{r}'}{|\mathbf{r}' - \mathbf{r}|} \tag{3}$$

Z_A is the charge on nucleus A, located at $\mathbf{R}_A$, and $\rho(\mathbf{r})$ is the electronic density. $V(\mathbf{r})$ is a physical observable and can also be measured experimentally, by electron or X-ray diffraction.[12−15] Its sign is any region depends on whether the positive contribution of the nuclei or the negative one of the electrons is dominant there. When $V(\mathbf{r})$ is evaluated on a molecular surface, we label it $V_S(\mathbf{r})$.

$V(\mathbf{r})$ and $V_S(\mathbf{r})$ have long been used in interpreting and predicting molecular reactive behavior,[13,14,16−22] particularly noncovalent interactions, e.g. hydrogen bonding.[23] The most negative values of $V_S(\mathbf{r})$, the surface local minima $V_{S,min}$, are usually associated with the lone pairs of electronegative atoms, such as nitrogen, oxygen and the halogens; they can also be found in the π-electron regions of unsaturated hydrocarbons.

One of the quantities in terms of which we characterize $V_S(\mathbf{r})$ is its average absolute deviation, which we denote by Π:

$$\Pi = \frac{1}{n}\sum_{i=1}^{n} |V_S(\mathbf{r}_i) - \bar{V}_S| \tag{4}$$

In eq 4, the summation is over the n points on a grid covering the molecular surface, and $\bar{V}_S$ is the overall average of $V_S(\mathbf{r})$:

$$\bar{V}_S = \frac{1}{n}\sum_{i=1}^{n} V_S(\mathbf{r}_i) \tag{5}$$

Π is a measure of the internal charge separation that is present in any molecule, even if its dipole moment is zero due to symmetry, e.g. *para*-dinitrobenzene. We have demonstrated that Π correlates with several empirical polarity scales.[24,25]

The average local ionization energy was originally introduced within the framework of Hartree−Fock theory:[26]

$$\bar{I}(\mathbf{r}) = \sum_i \frac{\rho_i(\mathbf{r})|\epsilon_i|}{\rho(\mathbf{r})} \tag{6}$$

In eq 6, $\rho_i(\mathbf{r})$ is the electronic density of the ith occupied atomic or molecular orbital and ϵ_i is its energy. We view $\bar{I}(\mathbf{r})$ as the average energy needed to remove an electron at the point $\mathbf{r}$ in the space of an atom or molecule, the focus being upon the point $\mathbf{r}$ and not a particular orbital.[26] This interpretation is based upon Hartree−Fock theory and Koopmans' theorem;[27] however, it has been shown to be qualitatively applicable to Kohn−Sham density functional results as well.[28]

$\bar{I}(\mathbf{r})$ and its molecular surface version $\bar{I}_S(\mathbf{r})$ are related to a number of fundamental atomic and molecular properties, as has been reviewed on two occasions;[29,30] these include shell structure, local temperature, electronegativity, local polarizability and bond strain. With respect to reactivity, the local minima of $\bar{I}_S(\mathbf{r})$, the $\bar{I}_{S,min}$, reveal the sites of the most energetic electrons, most readily transferred to electrophiles.[26,28,31−33] Indeed, $V_S(\mathbf{r})$ and $\bar{I}_S(\mathbf{r})$ can often be utilized in a complementary fashion, the minima of the former (its most negative values) showing where an approaching electrophile will initially be attracted and those of the latter indicating where are the most available electrons.[32,33]

Results

Figure 1 presents the potential energy and reaction force profiles along the intrinsic reaction coordinate of the process in eq 2. The position of the transition state is indicated by β; the minimum and maximum of $\mathbf{F}(\mathbf{R}_c)$ are at α and γ, respectively.

Table 1 presents the calculated geometries, the energy minima at 0 K and the enthalpies at 298 K for the isolated ground-state reactants and products and for the systems corresponding to $R_c = \alpha$, β, and γ. The structures of the latter three are shown in Figure 2. The transition state differs from that expected for an S_N2 attack by an ionic nucleophile, such as OH^-, which would be approaching a planar methyl group on the side opposite to the departing Cl^-.[10]

Energetics related to the reaction in eq 2, as determined from the data in Table 1, are given in Table 2. The overall ΔH(298 K) for the process is predicted to be +3.8 kcal/mol, compared to +7.7 kcal/mol obtained from experimental gas phase heats of formation.[34] The discrepancy of 3.9 kcal/mol is consistent with what would be expected at this computational level.[35]

TABLE 1: Structures and Energies Computed at the B3LYP/6-31G* Level[b]

system	distance, Å	angle, deg	E_{min}(0 K), hartrees	H(298 K), hartrees
H_3C-Cl	C−H: 1.090 (1.090) C−Cl: 1.804 (1.785)	H−C−H: 110.4 (110.8) H−C−CI: 108.5	−500.10854	−500.06645
H_2O	O−H: 0.969 (0.958)	H−O−H: 103.7 (104.5)	−76.40895	−76.38401
H_3C-OH	C−H: 1.094−1.101 (1.0936) C−O: 1.418 (1.4246) O−H: 0.969 (0.9451)	H−C−H: 108.0−108.4 (108.63) C−O−H: 107.7 (108.53)	−115.71441	−115.65870
HCl	H−Cl: 1.290 (1.2746)		−460.79569	−460.78572
$R_c = \alpha$	C−Cl: 2.280 C−O: 2.545 O-H_1: 0.970 O−H_2: 0.972 Cl−H_2: 2.203 C−H: 1.077−1.084 O−H_3: 1.896	H−C−H: 115−119 C−O−H_1: 104.0 H−O−H: 102.3 O−H_2−Cl: 130.6	−576.47442	−576.40908
$R_c = \beta$	C−Cl: 2.598 C−O: 2.172 O−H_1: 0.974 O−H_2: 0.995 Cl−H_2: 2.033 C−H: 1.079−1.080 O−H_3: 2.139	H−C−H: 117 C−O−H_1: 102.9 H−O−H: 102.3 O−H_2−Cl: 136.9	−576.43458	−576.36748
$R_c = \gamma$	C−Cl: 2.740 C-O: 1.760 O−H_1: 0.979 O−H_2: 1.165 Cl−H_2: 1.682 C−H: 1.083−1.087 O−H_3: 2.207	H−C−H: 113−117 C-O-H_1: 105.8 H−O−H: 102.6 O−H_2−Cl: 149.7	−576.46953	−576.40512

[a] Reference 38. [b] Experimental values, when available,[a] are in parentheses. The numbering of the hydrogens in the systems at $R_c = \alpha$, β and γ is shown in Figure 2.

TABLE 2: Computed Energetics (B3LYP/6-31G*) of the Reaction $CH_3Cl + H_2O \rightarrow CH_3OH + HCl$[b]

R → P (overall)	ΔE_{min}(0 K) = +4.6	ΔH(298 K) = +3.8 (+7.7)[a]
R → β	E_{act}(0 K) = +52.0	H_{act}(298 K) = +52.1
R → α	ΔE_{min}(0 K) = +27.0	ΔH(298 K) = +26.0
α → β	ΔE_{min}(0 K) = +25.0	ΔH(298 K) = +26.1
β → γ	ΔE_{min}(0 K) = −21.9	ΔH(298 K) = −23.6
γ → P	ΔE_{min}(0 K) = −25.5	ΔH(298 K) = −24.7

[a] Experimental, from gas phase heats of formation in ref 34. [b] Values are in kcal/mol.

Figure 1 shows that the traditional activation energy E_{act} can be viewed as a sum of two contributions:[6,8,9]

$$E_{act}(0\text{ K}) = -\int_R^\beta \mathbf{F}(\mathbf{R}_c)\,d\mathbf{R}_c = -\int_R^\alpha \mathbf{F}(\mathbf{R}_c)\,d\mathbf{R}_c - \int_\alpha^\beta \mathbf{F}(\mathbf{R}_c)\,d\mathbf{R}_c = \Delta E_{min}(0\text{ K}, R \rightarrow \alpha) + \Delta E_{min}(0\text{ K}, \alpha \rightarrow \beta) \quad (7)$$

The two components of E_{act}(0 K) and H_{act}(298 K) can be evaluated from the energies and enthalpies of the reactants and the systems at $R_c = \alpha$ and $R_c = \beta$, which are in Table 1. The results, in Table 2, show that, for this reaction, the energetic requirements for the preparation step, R → α, and for the first phase of the transition, α → β, are approximately the same: ΔE_{min}(0 K, R → α) = +27.0 kcal/mol and ΔE_{min}(0 K, α → β) = +25.0 kcal/mol, giving E_{act}(0 K) = +52.0 kcal/mol. Analogously, the second phase of the transition releases nearly as much energy as the relaxation to products, ΔE_{min}(0 K, β → γ) = −21.9 kcal/mol vs ΔE_{min}(0 K, γ → P) = −25.5 kcal/mol. It should not be inferred, however, that the two components of the energy changes before and after the transition state are typically so similar; this is often not the case.[4−6,8,9]

In Figures 3−5 can be seen the variation along the intrinsic reaction coordinate of some key features of the electrostatic potential and the average local ionization energy of the reaction system, computed on the molecular surfaces. The two negative centers are the oxygen and the chlorine atoms, and parts a and b of Figure 3 follow the changes in the most negative potentials

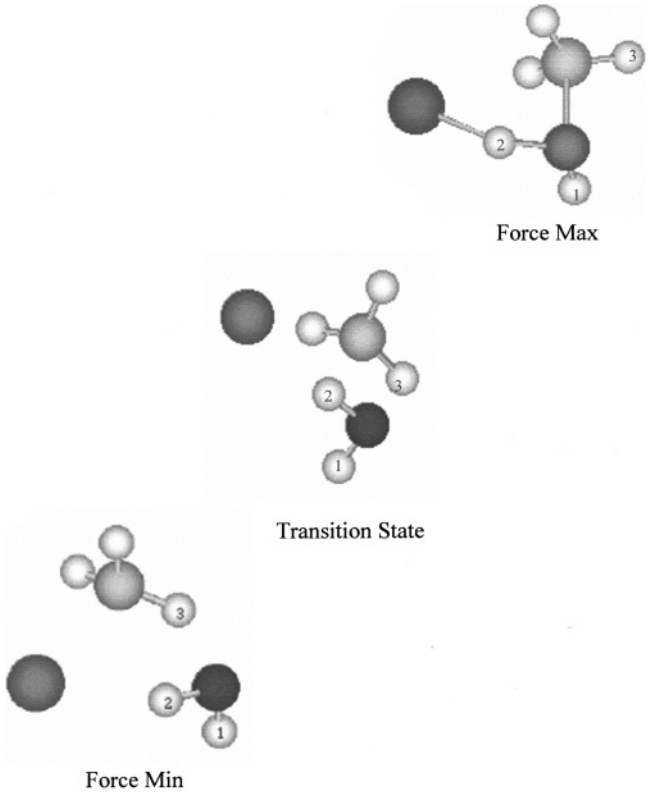

Figure 2. Structure of system at the three key points along the intrinsic reaction coordinate of the process in eq 2. The darkest sphere represents the oxygen, the lightest the carbon. The hydrogens mentioned in the text are numbered.

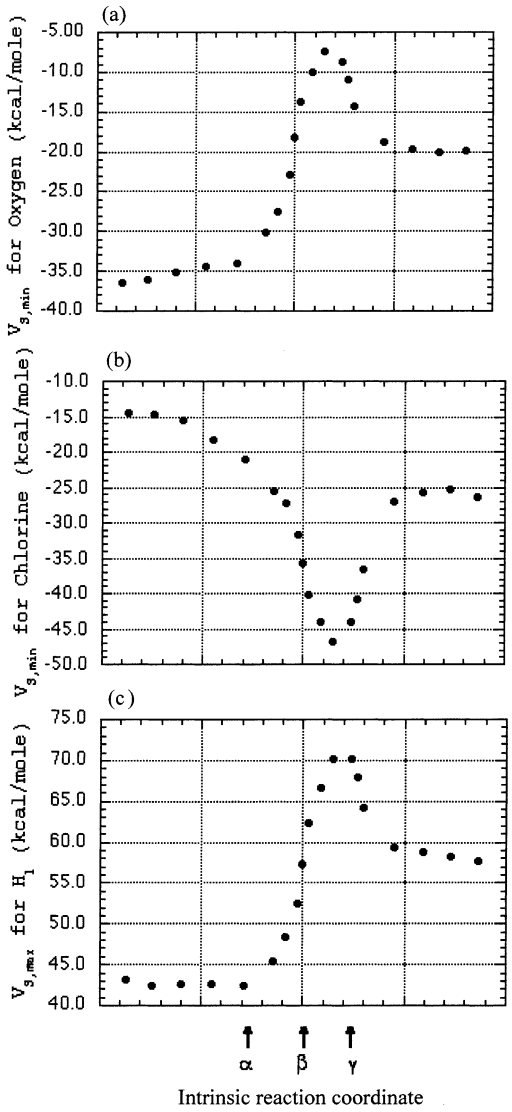

Figure 3. Variation of (a) $V_{S,min}$ of oxygen, (b) $V_{S,min}$ of chlorine, and (c) $V_{S,max}$ of hydrogen H_1 along intrinsic reaction coordinate. The positions of the reaction force minimum and maximum, α and γ, and the transition state, β, are indicated.

on them, their $V_{S,min}$. Hydrogens are normally positive; accordingly Figure 3c shows the most positive potential, $V_{S,max}$, on the hydrogen (H_1) that remains bonded to oxygen throughout the process. In parts a and b of Figure 4 are shown the lowest local ionization energies, the $\bar{I}_{S,min}$, on the oxygen and the chlorine. The relationship between $V_{S,min}$ and $\bar{I}_{S,min}$ for a given atom should be noted; their profiles along $\mathbf{R}_c$ are nearly superposable. As pointed out earlier,[5] this is because as an atomic region becomes more negative, the most energetic electron is less tightly held, and thus its ionization energy is lowered. Increasing positive character has the opposite effect. Finally, Figure 5 depicts the internal charge separation, $\prod$, during the reaction.

Discussion

The trends in the electronic properties shown in Figures 3−5 emphatically underscore the significance of the minimum and the maximum of $\mathbf{F}(\mathbf{R}_c)$ as indicators of different phases of a process. Starting with the reactants, each property initially changes relatively slowly and gradually. However at $R_c = \alpha$, the minimum of $\mathbf{F}(\mathbf{R}_c)$, begins a very rapid increase or decrease which continues until $R_c = \gamma$, the maximum of $\mathbf{F}(\mathbf{R}_c)$. Then

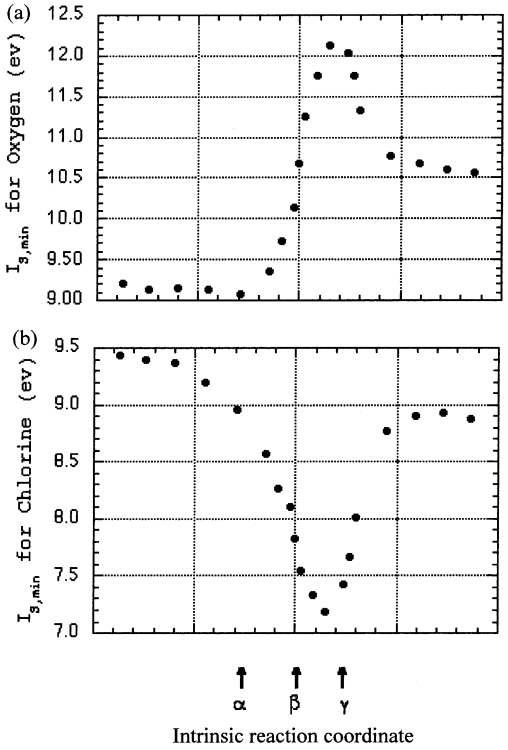

Figure 4. Variation of $\bar{I}_{S,min}$ of (a) oxygen and (b) chlorine along intrinsic reaction coordinate. The positions of the reaction force minimum and maximum, α and γ, and the transition state, β, are indicated.

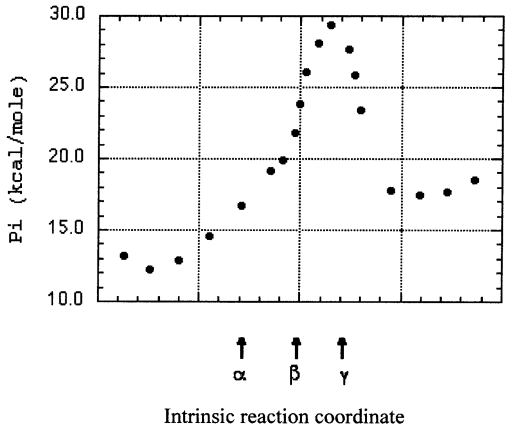

Figure 5. Variation of internal charge separation $\prod$ along intrinsic reaction coordinate. The positions of the reaction force minimum and maximum, α and γ, and the transition state, β, are indicated.

the property changes direction, and quite soon achieves an approximately constant value.

More specifically, the electrostatic potential of the oxygen in water is quite negative, $V_{S,min} = -37$ kcal/mol, Figure 3a. At $R_c = \alpha$, it is still −34 kcal/mol. Now, however, it quickly becomes much more positive, reaching $V_{S,min} = -7$ kcal/mol at $R_c = \gamma$, before leveling off to −20 kcal/mol in methanol. The chlorine potential behaves in an analogous but opposite manner, Figure 3b, starting with $V_{S,min} = -14$ kcal/mol in methyl chloride, progressing to −21 kcal/mol at $R_c = \alpha$ and then going all the way to −47 kcal/mol near $R_c = \gamma$ prior to settling to −27 kcal/mol in hydrogen chloride. These patterns are essentially duplicated by the local ionization energies of the oxygen and the chlorine; their $\bar{I}_{S,min}$ increase as the atom becomes more positive, and vice versa (Figure 4).

In physical terms, what is taking place in the four reaction zones defined by the points $R_c = \alpha$, β, and γ? Some insight

into this can be obtained by looking at the structural details in Table 1 and Figure 2.

In the first stage of the reaction, R → α, the primary effects are within the methyl chloride. The C−CI bond lengthens from 1.804 to 2.280 Å, and the methyl group moves toward planarity, the H−C−H angles increasing from 110 to 115−119°. (Planarity would correspond to angles of 120°.) The geometry of the water molecule is essentially unchanged from that in its isolated equilibrium state. However there are two intermolecular hydrogen bonds at $R_c = \alpha$, Cl- - -H_2 and O- - -H_3; this is confirmed by the respective separations, 2.203 and 1.896 Å.[36] The Cl- - -H_2 interaction is one of the factors causing the transition state to differ from that found for an ionic nucleophile like OH^-.[10] For the electronic properties in Figures 3−5, the consequences of the changes that occur in going from R to α are relatively minor.

The dominant event in this preparatory phase of the reaction is the stretching of the C−Cl bond by 0.476 Å. This produces an increasing retarding force, which reaches its extreme at $R_c = \alpha$, the minimum of $\mathbf{F}(\mathbf{R}_c)$. The preponderant role of this C−Cl lengthening can be seen by applying the Morse potential[37] to estimate the energy needed for this. Using the experimental H_3C−Cl force constant, 3.44 N/cm,[38] and taking the computed bond energy, 84.1 kcal/mol, the energy required to stretch the C−Cl bond by 0.476 Å is 26 kcal/mol. This is very close to our calculated ΔE_{min}(0 K, R → α) of 27 kcal/mol.

Moving now to the second reaction zone, between $R_c = \alpha$ and $R_c = \beta$, what is most notable is that the C−O bond starts to form, the effect of which begins to counter the retarding force. The C−O distance decreases from 2.545 to 2.172 Å. Internally, the H_20 molecule is still largely unaffected. The chlorine moves farther away from the carbon, and its hydrogen bond to H_2 is strengthened. As the reaction proceeds from $R_c = \beta$ to $R_c = \gamma$, the C−O and Cl−H_2 bonds continue to develop and now, finally, the O−H_2 lengthens, to 1.165 Å. At $R_c = \gamma$, the reacting portion of the system can be described as linked by three stretched covalent bonds: C−O−H_2−Cl. The formation of the C−O and Cl−H_2 bonds has been a driving force that, after $R_c = \beta$, becomes dominant. It reaches its maximum at $R_c = \gamma$.

During these processes, the electrostatic potentials associated with the oxygen, its noninteracting hydrogen (H_1), and the chlorine all change considerably, and very rapidly (Figure 3). The $V_{S,min}$ of the oxygen becomes much less negative, while that of the chlorine does the reverse. The $V_{S,max}$ of H_1 becomes strongly positive. All three reach their extremes at $R_c = \gamma$. In interpreting these results, it should be recalled from eq 3 that the $V_{S,min}$ and $V_{S,max}$ reflect both electronic and nuclear charges. For example, the $V_{S,min}$ of oxygen is due to the electronic density in its vicinity plus the positive contributions of its own and other nearby nuclei. Thus, an important factor in the oxygen's $V_{S,min}$ becoming less negative between $R_c = \alpha$ and $R_c = \gamma$ is its increasing proximity to the nuclei of the carbon and the methyl hydrogens. This also helps to explain the stronger $V_{S,max}$ of H_1. In contrast, the chlorine's moving away from the methyl group has the opposite effect upon its $V_{S,min}$.

Why do the trends in the $V_{S,min}$ of the oxygen and the chlorine and the $V_{S,max}$ of H_1 reverse directions at $R_c = \gamma$? A plausible explanation is the large internal charge separation that has developed. Figure 5 shows that $\prod$ reaches nearly 30 kcal/mol near $R_c = \gamma$, which—in our experience, involving several hundred molecules—is surpassed only by the zwitterions of two amino acids, glycine and histidine.[39] Pauling postulated in 1948 that systems try to minimize charge separation,[40] and this concept has been invoked in interpreting the sensitivities of energetic materials,[41,42] aqueous acidities,[43] etc.

We suggest, therefore, that a key component of the driving force after $R_c = \gamma$ is a tendency to diminish charge separation. This is accomplished in part by H_2 breaking away from the oxygen, causing the $V_{S,min}$ of the latter to become more negative and the $V_{S,max}$ of H_1 less positive. At the same time, the C−O and Cl−H_2 distances relax to their equilibrium values, the chlorine $V_{S,min}$ thereby becoming less negative.

A very striking feature of the transition state (at $R_c = \beta$) is that it marks the greatest rate of change (increase or decrease) for each of the properties shown in Figures 3−5 (between $R_c = \alpha$ and $R_c = \gamma$). Of course the transition state also has the universal significance of being the maximum of $V(\mathbf{R}_c)$ and a zero of $\mathbf{F}(\mathbf{R}_c)$.

Concluding Remarks

The minimum, zero, and maximum of the reaction force $\mathbf{F}(\mathbf{R}_c)$ provide an effective and universal basis for gaining insight into a chemical process. The maximum and minimum, and sometimes the zero,[5] show where distinct phases of the reaction begin and end, and where marked changes occur in the variation of certain structural and electronic properties. These frequently increase or decrease quite gradually in the initial and final phases of the process, but much more rapidly between the minimum and maximum of the reaction force, the greatest rate of change being at the transition state. The particular properties that show this behavior may differ from one reaction to another, but the features of $\mathbf{F}(\mathbf{R}_c)$ represent a unifying approach to their analyses.

Acknowledgment. This study was supported by Charles University grants GAUK 181/2004/B_CH/MFF, and NSF-MŠMT ČR 1P05ME784 grant (J.V.B.). Special thanks are given to the computational resources from the University Meta-Centre of Charles University in Prague.

References and Notes

(1) Fukui, K. *Acc. Chem. Res.* **1981**, *14*, 363.
(2) Gonzalez, C.; Schlegel, H. B. *J. Phys. Chem.* **1990**, *94*, 5523.
(3) Toro-Labbé, A. *J. Phys. Chem. A* **1999**, *103*, 4398.
(4) Jaque, P.; Toro-Labbé, A. *J. Phys. Chem. A* **2000**, *104*, 995.
(5) Toro-Labbé, A.; Gutiérrez-Oliva, S.; Concha, M. C.; Murray, J. S.; Politzer, P. *J. Chem. Phys.* **2004**, *121*, 4570.
(6) Herrera, B.; Toro-Labbé, A. *J. Chem. Phys.* **2004**, *121*, 7096.
(7) Martinez, J.; Toro-Labbé, A. *Chem. Phys. Lett.* **2004**, *392*, 132.
(8) Gutiérrez-Oliva, S.; Herrera, B.; Toro-Labbé, A.; Chermette, H. *J. Phys. Chem. A* **2005**, *109*, 1748.
(9) Politzer, P.; Toro-Labbé, A.; Gutiérrez-Oliva, S.; Herrera, B.; Jaque, P.; Concha, M. C.; Murray, J. S. *J. Chem. Sci.* **2005**, in press.
(10) March, J. *Advanced Organic Chemistry*, 3rd ed.; Wiley-lnterscience: New York, 1985.
(11) Bader, R. F. W.; Carroll, M. T.; Cheeseman, J. R.; Chang, C. *J. Am. Chem. Soc.* **1987**, *109*, 7968.
(12) Stewart, R. F. *J. Chem. Phys.* **1972**, *57*, 1664.
(13) Politzer, P.; Truhlar, D. G., Eds. *Chemical Applications of Atomic and Molecular Electrostatic Potentials*; Plenum Press: New York, 1981.
(14) Náray-Szabó, G.; Ferenczy, G. G. *Chem. Rev.* **1995**, *95*, 829.
(15) Feil, D. In: *Molecular Electrostatic Potentials: Concepts and Applications*; Murray, J. S., Sen, K., Eds.; Elsevier: Amsterdam, 1996, Chapter 13.
(16) Scrocco, E.; Tomasi, J. *Adv. Quantum Chem.* **1978**, *11*, 115.
(17) Politzer, P.; Daiker, K. C. In: *The Force Concept in Chemistry*; Deb, B. M., Ed.; Van Nostrand Reinhold: New York, 1981, Chapter 6.
(18) Politzer, P.; Laurence, P. R.; Jayasuriya, K. *Environ. Health Perspect.* **1985**, *61*, 191.
(19) Politzer, P.; Murray, J. S. In *Reviews in Computational Chemistry*; Lipkowitz, K., Boyd, D. B., Eds.; VCH: New York, 1991; Vol. 2, Chapter 7.
(20) Politzer, P.; Murray, J. S.; Peralta-Inga, Z. *Int. J. Quantum Chem.* **2001**, *85*, 676.
(21) Murray, J. S.; Politzer, P. *J. Mol. Struct. (THEOCHEM)* **1998**, *425*, 107.

(22) Politzer, P.; Murray, J. S. *Trends Chem. Phys.* **1999**, *7*, 157.
(23) Hagelin, H.; Brinck, T.; Berthelot, M.; Murray, J. S.; Politzer, P. *Can. J. Chem.* **1995**, *73*, 483.
(24) Brinck, T.; Murray, J. S.; Politzer, P. *Mol. Phys.* **1992**, *76*, 609.
(25) Murray, J. S.; Brinck, T.; Lane, P.; Paulsen, K.; Politzer, P. *J. Mol. Struct. (THEOCHEM)* **1994**, *307*, 55.
(26) Sjoberg, P.; Murray, J. S.; Brinck, T.; Politzer, P. *Can. J. Chem.* **1990**, *68*, *8*, 1440.
(27) Koopmans, T. A. *Physica* **1933**, *1*, 104.
(28) Politzer, P.; Abu-Awwad, F.; Murray, J. S. *Int. J. Quantum Chem.* **1998**, *69*, 607.
(29) Murray, J. S.; Politzer, P. In *Theoretical Organic Chemistry*; Parkányi, C., Ed.; Elsevier: Amsterdam, 1998, Chapter 7.
(30) Politzer, P.; Murray, J. S. In *Theoretical Aspects of Chemical Reactivity*; Toro-Labbé, A., Ed.; Elsevier: Ámsterdam, in press.
(31) Brinck, T.; Murray, J. S.; Politzer, P. *Int. J. Quantum Chem.* **1993**, *48*, 73.
(32) Murray, J. S.; Peralta-Inga, Z.; Politzer, P.; Ekanayake, K.; LeBreton, P. *Int. J. Quantum Chem.* **2001**, *83*, 245.
(33) Politzer, P.; Murray, J. S.; Concha, M. C. *Int. J. Quantum Chem.* **2002**, *88*, 19.
(34) Mallard, W. G., Linstrom, P. J., Eds. *NIST Chemistry Webbook*, NIST Standard Reference Database No. 69; NIST: Gaithersburg, MD, 1998; http://webbook.nist.gov.
(35) Curtiss, L. A.; Raghavachari, K.; Redfern, P. C.; Pople, J. A. *J. Chem. Phys.* **2000**, *112*, 7374.
(36) Hamilton, W. C.; Ibers, J. A. *Hydrogen Bonding in Solids*; W. A. Benjamin: New York, 1968.
(37) Levine, I. N. *Quantum Chemistry*, 5th ed.; Prentice Hall: Upper Saddle River, NJ, 2000.
(38) Lide, D. R. *Handbook of Chemistry and Physics*, 78th ed.; CRC Press: New York, 1997.
(39) Murray, J. S.; Peralta-Inga, Z.; Politzer, P. *Int. J. Quantum Chem.* **2000**, *80*, 1216.
(40) Pauling, L. *J. Chem. Soc.* **1948**, 1461.
(41) Murray, J. S.; Lane, P.; Politzer, P. *Mol. Phys.* **1998**, *93*, 187.
(42) Politzer, P.; Murray, J. S. In *Energetic Materials. Part 2. Detonation, Combustion*; Politzer, P., Murray, J. S., Eds.; Elsevier: Amsterdam, 2003; Chapter 1.
(43) Ma, Y.; Gross, K. C.; Hollingsworth, C. A.; Seybold, P. G.; Murray, J. S. *J. Mol. Mod.* **2004**, *10*, 235.